Mathematical Geology, Vol. 20, No. 7, 1988

Spatial and Multivariate Analysis of Geochemical Data from Metavolcanic Rocks in the Ben Nevis Area, Ontario[1]

E. C. Grunsky[2] and F. P. Agterberg[3]

A study of the lithogeochemistry of metavolcanics in the Ben Nevis area of Ontario, Canada has shown that factor analysis methods can distinguish lithogeochemical trends related to different geological processes, most notably, the principal compositional variation related to the volcanic stratigraphy and zones of carbonate alteration associated with the presence of sulphides and gold. Auto- and cross-correlation functions have been estimated for the two-dimensional distribution of various elements in the area. These functions allow computation of spatial factors in which patterns of multivariate relationships are dependent upon the spatial auto- and cross-correlation of the components. Because of the anisotropy of primary compositions of the volcanics, some spatial factor patterns are difficult to interpret. Isotropically distributed variables such as CO_2 are delineated clearly in spatial factor maps. For anisotropically distributed variables (SiO_2), as the neighborhood becomes smaller, the spacial factor maps becomes better. Interpretation of spatial factors requires computation of the corresponding amplitude vectors from the eigenvalue solution. This vector reflects relative amplitudes by which the variables follow the spatial factors. Instability of some eigenvalue solutions requires that caution be used in interpreting the resulting factor patterns. A measure of the predictive power of the spatial factors can be determined from autocorrelation coefficients and squared multiple correlation coefficients that indicate which variables are significant in any given factor. The spatial factor approach utilizes spatial relationships of variables in conjunction with systematic variation of variables representing geological processes. This approach can yield potential exploration targets based on the spatial continuity of alteration haloes that reflect mineralization.

KEY WORDS: auto-correlation, cross-correlation, lithogeochemistry, multiple correlation coefficients, trend eigenvector, amplitude eigenvector.

INTRODUCTION

Volcanic rocks frequently host several types of mineral deposits such as syngenetic polymetallic massive sulfides and epigenetic precious metal deposits. Alteration of the volcanic host rocks occurs from passage of hydrothermal fluids

[1]Manuscript received 31 August 1987; accepted 30 October 1987.

[2]Ontario Geological Survey, 77 Grenville Street, Toronto, Ontario, Canada.

[3]Geological Survey of Canada, 601 Booth Street, Ottawa, Ontario, Canada.

0882-8121/88/1000-0825$06.00/1

associated with the mineralizing event and is discernible because of mineralogical, textural, and chemical changes. Most deposits are surrounded by haloes of alteration that are defined by anomalous chemical signatures. These zones are spatially much larger than the ore deposits and thus are significant exploration targets. Lithogeochemistry can be instrumental in detecting these alteration zones when statistical techniques are used to recognize patterns of alteration. The application of multivariate methods provides a quantitative and concise means by which systematic variation of lithogeochemical data can be described. Because lithogeochemistry of igneous rocks reflects geological processes that have acted in forming or altering the rock, multivariate methods can assist in delineating these effects.

The Ben Nevis area of Ontario in the Abitibi Volcanic Belt of the Canadian Shield (Fig. 1), contains an occurrence of gold, silver, copper, zinc, and lead mineralization surrounded by a larger zone of carbonatized volcanic rocks. Mineralization of the Canagua Mines Property appears to be of an epigenetic vein type origin. Another significant occurrence is the Croxall property northwest of Verna Lake (Fig. 1). This occurrence consists of a zone of brecciated and sheared rhyolite with interstitial pyrite, chalcopyrite, chlorite, calcite, and quartz. Gold assays up to 1 ppm have been reported. A smaller zone of sericitic and pyritic alteration also surrounds this occurrence. Several other sulfide-rich zones occur throughout the map area. Some occurrences have small alteration zones and some have no alteration associated with them. Details on the occurrences and geology can be found in Jensen (1975). A later study (Grunsky, 1986) of the lithogeochemical data (39 chemical components per sample) combined with correspondence analysis and dynamic cluster analysis outlined the compositionally distinct volcanic units (Fig. 2), zones of carbonate alteration, sulfur enrichment, and other lithogeochemically anomalous zones. For exam-

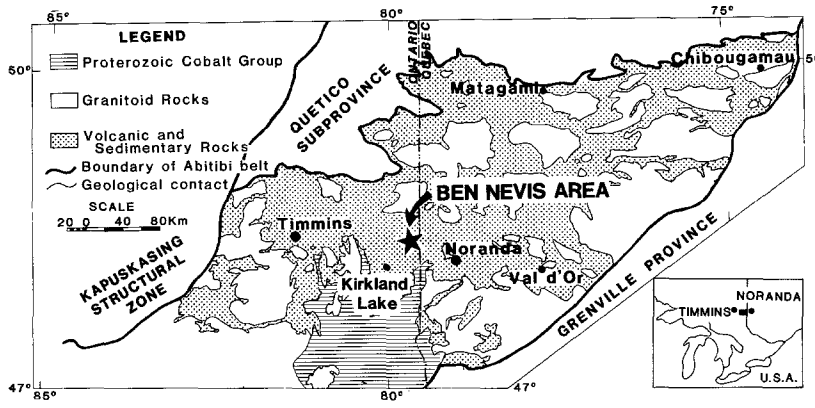

Fig. 1. Location of Ben Nevis study area.

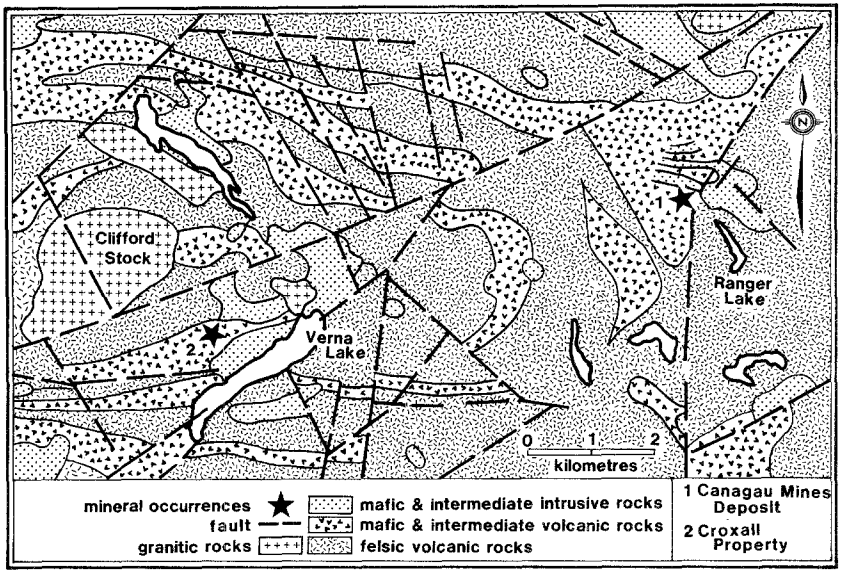

Fig. 2. General geologic map of Ben Nevis area.

ple, the second factor in correspondence analysis has large weight for CO_2, and delineates the carbonate alteration zones.

The purpose of the present study is to consider spatial auto- and cross-correlation of lithogeochemical data previously subjected to multivariate analysis. Auto- and cross-correlation functions describe the variation of a variable over an interval of measurement, in this case distance. Functions used in this paper are isotropic in that they describe variation in one direction only. Anisotropic variation of variables presents a more complex problem and is not dealt with here. Thus, by using isotropic statistical models for auto- and cross-correlation functions, the multivariate relationships between chemical constituents of volcanic rocks are based on neighborhoods of samples instead of individual samples only.

The presentation of spatial patterns for individual variables and factors is one of the most significant aspects of this type of study and is explained first. The distribution of the 825 samples used in the study (Fig. 3) is uneven, and a gridding process was used to estimate variables over a regular interval. All of the spatial patterns of oxides and multivariate factors and scores of the spatial factors of the experiments were gridded using the inverse distance-squared weighting function method (cf., Shepard, 1968). At each grid node, the eight nearest neighbors were included in grid estimation. This relatively simple contouring method has been used for presenting patterns of the original data in the next section as well as different types of factor scores in later sections. The

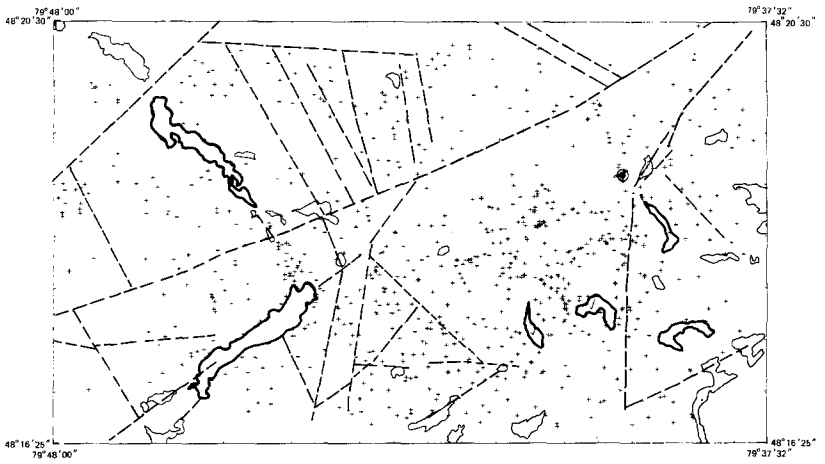

Fig. 3. Location map of samples in Ben Nevis area.

approximate dimensions of the area are 12.7 km east–west and 7.4 km north–south. The area was divided into a 40 × 40 grid such that dimensions of each grid cell are 320.0 × 195.0 m. Various grid sizes were tried; results indicated, as expected, that as grid cell dimensions increased, the detail of geochemical patterns decreased. Although, even in a grid size of 10 × 10, the major regional geochemical features still were evident. A grid size of 40 × 40 was considered the optimum size for the purpose of this study.

LITHOGEOCHEMICAL VARIATION IN THE BEN NEVIS AREA

Chemical patterns that variables exhibit reflect results of several geological processes. Si, Al, Fe, Mg, Ca, Na, and K lithogeochemical patterns generally reflect the compositional variation due to fractionation of the initial magma. Variation of Si in the map area (Fig. 4a) shows how Si abundance reflects volcanic rocks (Fig. 2) that contain varying amounts of Si. This pattern of compositional variation due to initial magma composition is exhibited by several variables and is the most dominant pattern in the area. Also, rock types that reflect this pattern can be mapped visually. Other variables such as Al, Ca, Na, and K usually reflect as well effects of other secondary processes (i.e., metamorphism, alteration). The overall compositional variation of Ca (Fig. 4b) is reflected in this pattern as well as other secondary effects related to alteration. Spatial variation of CO_2, S, and Li (Figs. 4c–4e) show hydrothermal alteration, and mineralization has resulted in larger patterns which surround the mineralized S-rich zones. Other components, such as Al, Ca, and K, also reflect alteration associated with mineralization. For example, Ca (Fig. 4b) shows a zone

of enrichment around the zone of carbonatization, and Al shows depletion. Sulfide-rich occurrences are observed readily in the map of S (Fig. 4d). The sizes of these zones are smaller than they actually appear because of gridding used to present the data. The more significant mineralized sulfide occurrences have associated alteration within the host rocks which does not show when looking only at the sulfur map. A multivariate approach might better assist in distinguishing the more significant exploration targets.

ELEMENT VARIATION PATTERNS DERIVED BY CORRESPONDENCE ANALYSIS

Correspondence analysis, a technique similar to principal components analysis, was applied previously to the Ben Nevis data and interpretation of factor scores was discussed then (Grunsky 1986). In order to provide a consistent interpretation, the method of correspondence analysis was reapplied to three sets of variables used in this study. These three sets of variables are:

a. A set of four variables, comprised of CO_2–S–Li–Zn, that represent alteration and mineralization in the area.

b. A set of seven variables comprised of Si–Al–Fe–Mg–Ca–Na–K, which represent primary compositional variation within the volcanic rocks. Secondary alteration effects occur mostly within Ca, Na, and K.

c) A set of nine variables consisting of Si–Al–Fe–Mg–Ca–Na–K–CO_2–Li, which reflect both primary compositional variation (Si–Al–Fe–Mg–Ca–Na–K) and alteration (K–CO_2–Li).

Results of the correspondence analysis for the set of four variables CO_2–S–Li–Zn show that CO_2, Li, and Zn contribute over 95% of the variation in the first factor and 61% of the total variation in the data. The second factor is dominated by S. Zones of sulfur enrichment correspond to sulfide zones associated with base and precious metal mineralization. The distribution of Zn reflects both base metal enrichment associated with sulfides and also the presence of the larger alteration zone that surrounds the Cu–Au mineralization.

Two major patterns emerge from this analysis (Fig. 5a); a pattern associated with large-scale alteration (CO_2, Li, Zn) and a pattern associated with locally enriched mineralized zones.

Results of the correspondence analysis on the seven-variable set shows that the first factor accounts for 58% of the total variation of the data. The first factor is dominated by contributions of Si, Al, Fe, Mg, and Ca (Fig. 5b). The second factor accounts for 20% of data variation and is dominated by Ca. The spatial pattern of factor 2 (not shown) indicates a zone of Ca enrichment (cf., Fig. 4b) around the zone of carbonatization. The third factor (12% of the data variation) is accounted for by variation of Mg and K enrichment associated with mafic intrusive rocks and K-rich rhyolitic rocks and alteration zones.

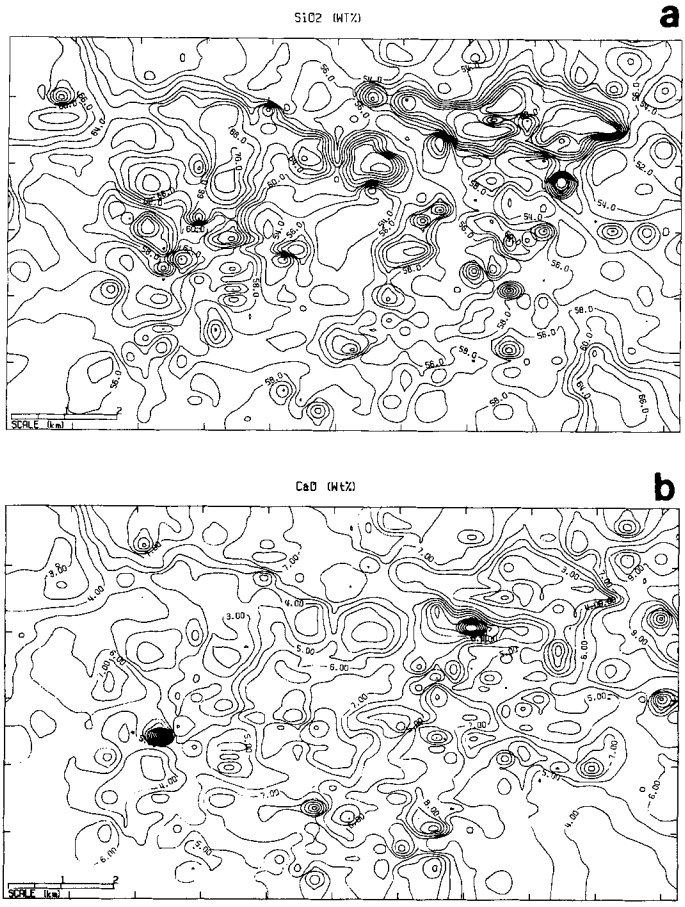

Fig. 4. (a) Map of SiO_2 in Ben Nevis area. SiO_2 typically reflects rock type in volcanic terrains. Note that the pattern of the map is similar to the geological map (Fig. 2). (b) Map of CaO in Ben Nevis area. Note that the pattern of the map outlines both compositional variation and a zone of Ca enrichment around the main zone of carbonate alteration. (c) Map of CO_2 in Ben Nevis area. An abundance of CO_2 greater than 1.0 wt % in volcanic rocks is indicative of alteration, and the zone of carbonatization associated with hydrothermal alteration is clearly shown. (d) Map of Sulfur in Ben Nevis area. S reflects local zones of mineralization, some of which are associated with hydrothermal alteration zones whereas others are not. (e) Map of Li in Ben Nevis area. Li enrichment is associated typically with hydrothermal systems. Li anomalies are similar to CO_2 anomalies.

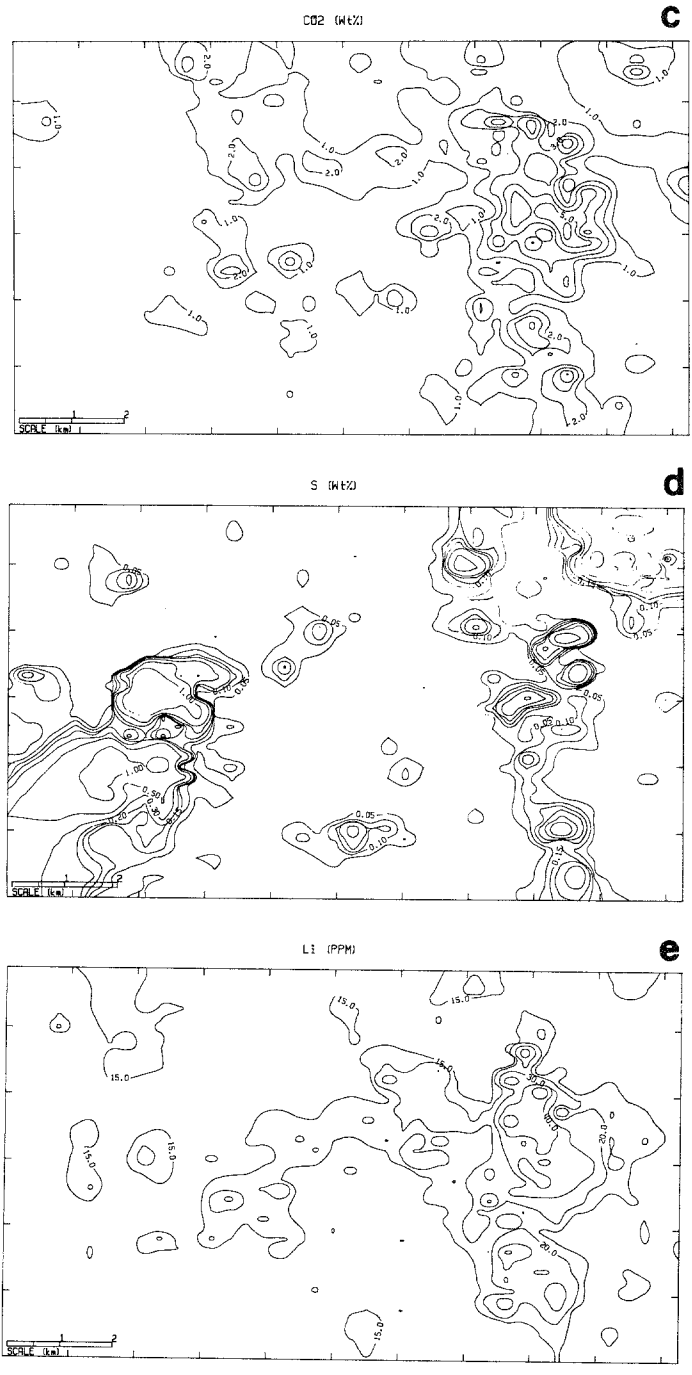

Fig. 4. Continued

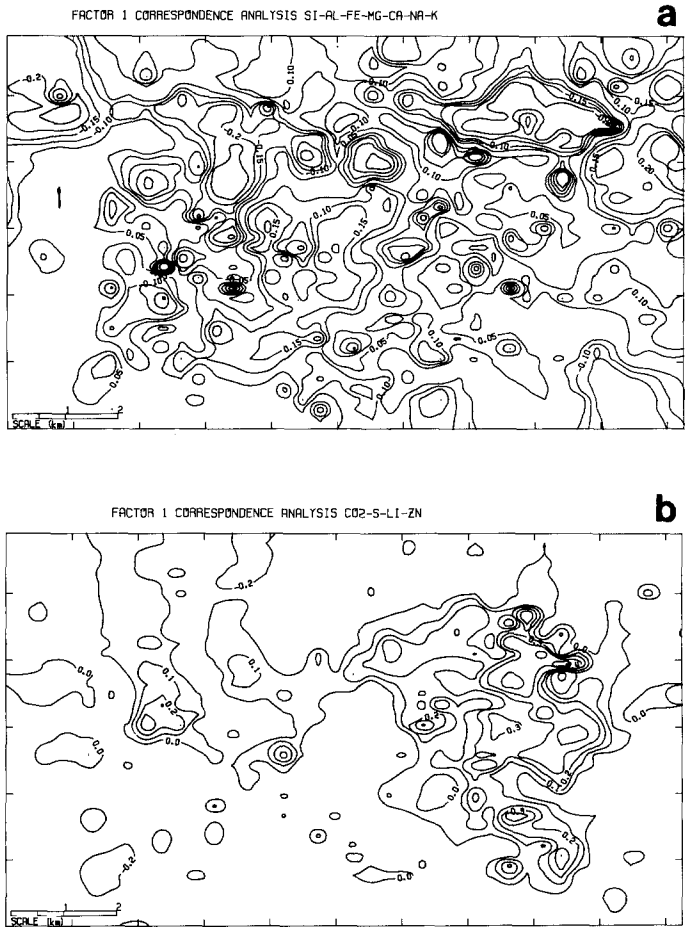

Fig. 5. (a) Factor 1 scores from correspondence analysis for the seven-variable case. This factor outlines compositional variation of the volcanics. (b) Factor 1 scores from correspondence analysis for the four-variable case. The main zone of carbonate alteration is outlined by this factor.

The nine-variable set of elements, when subjected to correspondence analysis, produced four significant factors that account for 53%, 22%, 12%, and 6% of the data, respectively. The first factor is dominated by variation of Li, Si, and CO_2 and produces a spatial pattern similar to Fig. 5a. The second factor is dominated by variation of Al, Fe, Mg, Ca, and K and reflects primary compositional variation of the volcanics with a spatial pattern similar to Figs. 5b and 4a. The third factor is dominated by a combination of Ca and CO_2 enrichment showing a pattern where both variables are combined. This spatial pattern

is similar to a combination of Figs. 4b,c. Factor 4 (not shown) shows the opposing relationships of Na and K that occur in close proximity to the mineralized zones.

SPATIAL AUTO- AND CROSS-CORRELATION

Various statistical models have been developed for estimating the auto- and cross-correlation of variables in space as described by Journel and Huijbregts (1978), Bennett (1979), and Upton and Fingleton (1985). Most of these methods are based on situations in which sampling points occur at regular intervals along lines or at nodes of a regular grid. Because of irregular distribution of outcrops in our study area, the sampling points are not at equal intervals (Fig. 3) and estimates obtained in this study have been determined from irregularly distributed points.

Areal distribution of samples must be considered when auto-correlation and cross-correlation functions are estimated. The problem of modeling spatial auto-correlation of residuals from polynomial trend surfaces has been discussed by Huijbregts and Matheron (1970), Delfiner (1975), and, more recently, Haining (1985). Models tested by Haining can be applied also to data from which trends have not been eliminated. A simple model for estimating a quadratic approximation to the autocorrelation function from irregularly spaced data originally proposed by Agterberg (1970) performed well in Haining's tests. The basis of the quadratic model and derivation of functions used in this model are outlined in Appendix A.

In this study, auto- and cross-correlation functions were estimated with neighborhood radii (D) varying from 50 m to 4 km (Table 1). The degree of fit of a parabola for a specific neighborhood is best in the vicinity of the average distance for this neighborhood.

Shapes of the parabolic functions (Fig. 6) and coefficients of estimated

Table 1. Average Sample Distances and Numbers Within Selected Neighborhoods

Neighborhood (m)	Average number of samples	Average sample distance
50	.4	18.4
100	1.1	55.6
250	4.2	149.3
500	13.6	309.5
1000	44.6	631.6
2000	154.6	1273.1
4000	421.0	2369.8

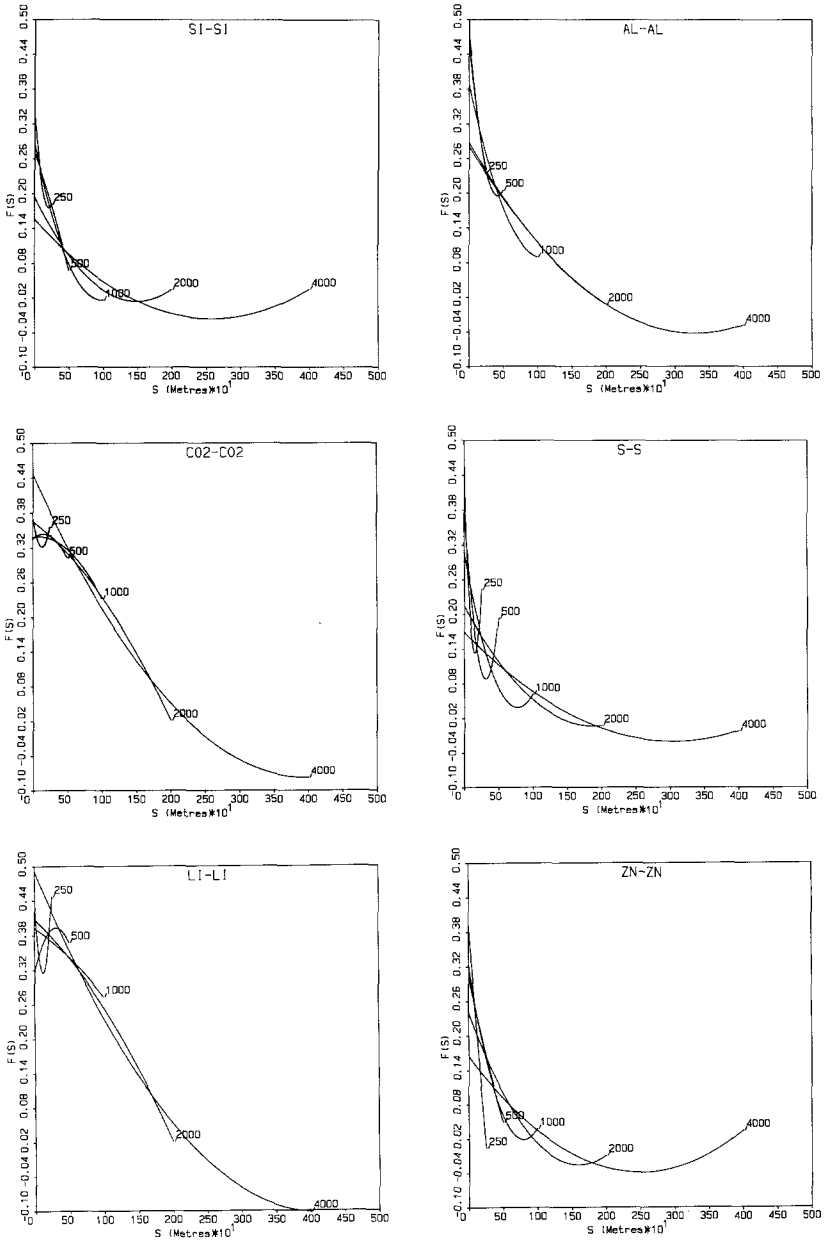

Fig. 6. Quadratic function approximation of the auto-correlation and cross-correlation functions for Si, Al, CO_2, S, Li, and Zn. Each curve terminates at the end of the neighborhood for which the function was calculated. The correlation coefficient (R) is shown as an asterisk on the y axis of the parabolic function curves. The first six curves (a)–(f), approximate auto-correlation functions. The remaining curves, (g) to (l), approximate cross-correlation functions of the variables. Not all variables used in the study are shown in these curves.

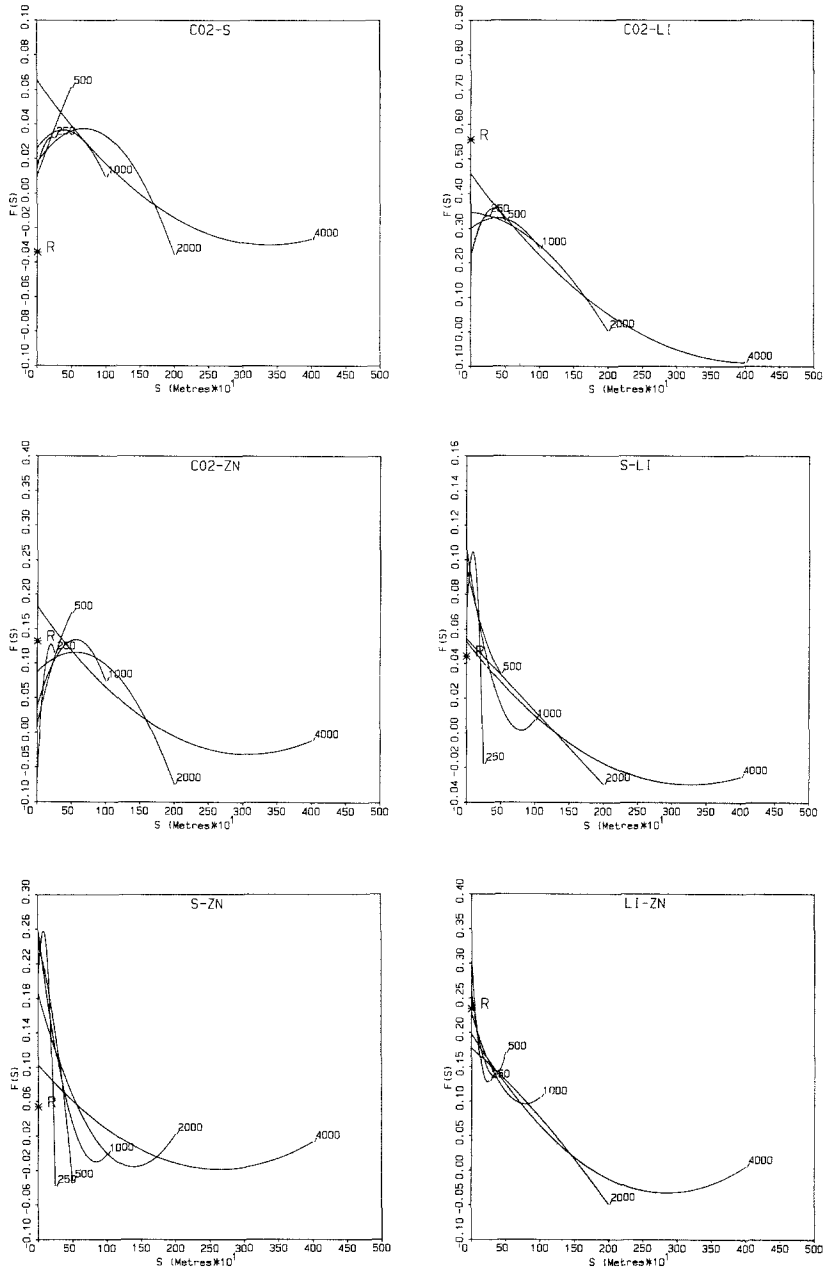

Fig. 6. Continued

Table 2. Auto/Cross-Correlation Coefficients

Autocorrelation coefficients

	Si-Si Coefficients			CO_2-CO_2 Coefficients		
Neighborhood	A	$B*X$	$C*X^2$	A	$B*X$	$C*X^2$
250.	.35002905	−.00165903	.00000395	.37507474	−.00076527	.00000275
500.	.27103460	−.00032546	−.00000016	.33522120	−.00010958	−.00000035
1000.	.28688642	−.00055850	.00000029	.33841121	.00002346	−.00000013
2000.	.19479574	−.00024118	.00000008	.36612883	−.00008893	−.00000004
4000.	.15599529	−.00013267	.00000003	.44675118	−.00026461	.00000003

	S-S Coefficients			Li-Li Coefficients		
Neighborhood	A	$B*X$	$C*X^2$	A	$B*X$	$C*X^2$
250.	.44571537	−.00398575	.00001271	.44000834	−.00202260	.00000821
500.	.38999817	−.00192112	.00000306	.31681520	.00048445	−.00000076
1000.	.30765647	−.00069744	.00000045	.39288762	−.00008181	−.00000004
2000.	.21431395	−.00022178	.00000006	.40857968	−.00011333	−.00000004
4000.	.16959698	−.00012425	.00000002	.49133605	−.00029038	.0000000

	Zn-Zn Coefficients		
Neighborhood	A	$B*X$	$C*X^2$
250.	.39444730	−.00161057	.00000020
500.	.30731270	−.00060191	.00000017
1000.	.32113951	−.00075676	.00000047
2000.	.24101809	−.00033361	.00000010
4000.	.16430871	−.00016236	.00000003

Crosscorrelation Coefficients

	Si-CO_2 and CO_2-Si Averaged coefficients			S-Si Averaged coefficients		
Neighborhood	A	$B*X$	$C*X^2$	A	$B*X$	$C*X^2$
250.	.05204545	.00075619	−.00000387	.24651165	−.00050872	−.00000167
500.	.11605299	−.00058276	.00000090	.23030779	−.00071020	.00000073
1000.	.07770173	−.00014910	.00000006	.20141356	−.00048352	.00000033
2000.	.03303507	−.00001784	.00000000	.12007903	−.00012998	.00000004
4000.	.02900602	−.00000353	.00000000	.09366345	−.00006613	.00000001

	Si-Li and Li-Si Averaged coefficients			Si-Zn and Zn Averaged coefficients		
Neighborhood	A	$B*X$	$C*X^2$	A	$B*X$	$C*X^2$
250.	−.04713026	.00245305	−.00001059	.05451455	.00251247	−.00001163
500.	.09296227	−.00057745	.00000078	.16177064	−.00015417	−.00000056
1000.	.05084213	−.00018231	.00000012	.18861033	−.00056788	.00000039
2000.	−00967754	.00003336	−.00000002	.08129474	−.00011721	.00000004
4000.	−.01189961	.00002691	−.00000001	.04195785	−.00003659	.00000001

Table 2. Continued

Neighborhood	CO_2–S and S–CO_2 Averaged coefficients A	B^*X	C^*X^2	CO_2–Li and Li–CO_2 Averaged coefficients A	B^*X	C^*X^2
250.	.01467544	.00015919	−.00000036	.21902244	.00096544	−.00000197
500.	.00952880	.00011460	−.00000002	.21893354	.00084671	−.00000128
1000.	.02599697	.00005519	−.00000007	.29982153	.00016699	−.00000022
2000.	.01759662	.00005798	−.00000004	.34697002	−.00002273	−.00000007
4000.	.06542861	−.00005655	.00000001	.45758158	−.00026864	.00000003

Neighborhood	CO_2–Zn and Zn–CO_2 Averaged coefficients A	B^*X	C^*X^2	S–Li and Li–S Averaged coefficients A	B^*X	C^*X^2
250.	−.06695214	.00194061	−.00000484	.06851044	.00082216	−.00000467
500.	.00871561	.00046083	−.00000026	.09509793	−.00018106	.00000012
1000.	.03624722	.00034957	−.00000031	.10598613	−.00025913	.00000016
2000.	.08736036	.00010264	−.00000009	.05441260	−.00004168	.00000000
4000.	.18206951	−.00013883	.00000002	.05276841	−.00005069	.00000001

Neighborhood	S–Zn and Zn–S Averaged coefficients A	B^*X	C^*X^2	Li–Zn and Zn–Li Averaged coefficients A	B^*X	C^*X^2
250.	.20238037	.00147146	−.00000973	.30718029	−.00154954	.00000335
500.	.24263397	−.00026885	−.00000056	.25826758	−.00074132	.00000113
1000.	.25701344	−.00063112	.00000037	.22879666	−.00033904	.00000022
2000.	.18580724	−.00028883	.00000010	.17716601	−00008871	−.00000001
4000.	.10216813	−.00009151	.00000002	.19826043	−.00016227	.00000003

Note: Model $Y = A + B^*X + C^*X^2$ using the Model $Y = A + B^*X + C^*X^2$

functions (Table 2) for selected chemical constituents, mainly SiO_2, CO_2, S, Li, and Zn provide approximations of unknown auto- and cross-correlation functions. The curves and coefficients are averaged for pairs of variables and are for standardized values of the elements. Means and standard deviations are shown (Table 3).

As models of estimation, parabolas do not fulfill some of the properties required by the auto-correlation function. The quadratic functions are not positive-definite, nor do they satisfy the Cauchy–Schwarz inequality. However within the range of use (i.e., neighborhood limits), values of the functions are within the required range ($-1 \leq r \leq 1$) so that the Cauchy–Schwarz inequality is satisfied. This can be observed in the curves (Fig. 6). Auto- and cross-correlation functions were also estimated using discrete lag intervals that normally

Table 3. Means, Standard Deviations, and Correlation Coefficients

	Mean	Std. Dev.	SiO_2	CO_2	S	Li	Zn
SiO_2	58.5594	7.4084	1.0000	.0000	.0000	.0000	.0000
CO_2	1.3223	1.8122	−.1262	1.0000	.0000	.0000	.0000
S	.1255	.4834	.0318	−.0342	1.0000	.0000	.0000
Li	17.0091	11.3595	−.3954	.5554	.0442	1.0000	.0000
Zn	88.7825	96.5587	−.0586	.1323	.0538	.2343	1.0000

are used to determine spatial covariances and the variance of lagged differences for the semi- and covariogram. Estimates of the auto- and cross-correlation functions, as well as estimates derived from the semi- and covariograms, for a given interval h are close to the value of the quadratic functions. This suggests that quadratic functions are good estimates of the auto- and cross-correlation. Also, these functions decay to zero as the lag (h) increases, which is equivalent to approaching the sill of the semivariogram, and this suggests that stationarity exists within the data. Because these quadratic functions, as models of auto- and cross-correlation functions, are not positive-definite, some cases occur in which the condition of positive-definiteness is violated. An adjustment algorithm (shown below) can be applied which ensures that this condition is met. This is considered in the next sections where auto- and cross-correlations for groups of four, seven, and nine variables are combined with one another.

The patterns suggested by the overlapping parabolas for auto-correlation are of two kinds: (1) exponential-type curves with a relatively steep slope at the origin (discontinuous first derivative) are indicated here by Si, Al, S, and Zn; and (2) gaussian-type curves which are horizontal at the origin (continuous first derivative) are shown by CO_2 and Li. The average cross-correlation functions are also of two kinds: (1) exponential-type decrease as exemplified by the Li–Zn cross-correlation; and (2) increase toward a maximum in the vicinity of 400 m before decrease toward larger distances is indicated most clearly by CO_2–Li. The second kind of cross-correlation is shown also by the originally fitted parabolas of this pair before coefficients were averaged.

A geological interpretation of the preceding auto- and cross-correlation patterns is as follows. Most chemical constituents such as Si are subject to abrupt changes in two-dimensional space at contacts between different rock types (Fig. 2). This results in exponential-type auto- and cross-correlation functions. Because of the east–west structural trend in the area, contacts between rock types are, on the average, more closely spaced in the north–south direction. The corresponding spatial correlation functions are therefore probably anisotropic. Exponential-type decreases such as for Si (Fig. 6a) are primarily determined by the frequency of contacts of the lithological units; this frequency has been averaged with respect to direction. On the other hand, Co_2, Li, S, and Zn

are characteristic of alteration patterns which tend to be isotropic. These constituents, primarily CO_2 and Li, are characterized by a spatial variability that changes more slowly and gradationally than the others such as Si. Regional zoning also is indicated for the alteration. The maximum cross-correlation of CO_2 and Li at about 400 m suggests existence of clusters of relatively large CO_2 values, occurring, on the average, at a distance of 400 m from clusters of relatively large lithium values. This suggestion is confirmed when the contour maps for CO_2 and Li (Figs. 4c, e) are compared with one another. Both patterns show a number of distinct small peaks, especially within the northern part of the area. Several CO_2 peaks occur at a distance of about 400 m from Li peaks closest to them.

SPATIAL FACTOR ANALYSIS

The spatial analysis of multivariate systems in petrology and geochemistry has been studied from different points of view by Agterberg (1966, 1974), Myers (1982, 1988), Royer (1984, 1988), Switzer and Green (1984), and Wackernagel (1985, 1988). Myers has developed methods of "cokriging" in order to perform multivariate prediction of values of variables at points from the same variables measured at other points in the neighborhood. Most authors first treated their data by existing methods of multivariate analysis such as principal components analysis or correspondence analysis in order to extract "factors" from a symmetric matrix C_0, which is usually a variance-covariance matrix or a correlation matrix. For spatial factor analysis, eigenvalues and eigenvectors of a matrix of the type $C_0^{-1}C_1$ usually are determined where C_1 is a distance-variance matrix, generally of differences between variables measured at points with a given distance between them. Royer (1984) and Switzer and Green (1984) obtained linear combinations of variables which show continuous spatial variability versus "noise" components that are linear combinations without significant positive spatial correlation. Wackernagel (1985) first extracted a "noise" component from each individual variable before obtaining linear combinations for signal components of the variables. Our method of spatial factor analysis for the Ben Nevis area is explained in detail in the next section. It differs from earlier applications in Agterberg (1966, 1974) in the following ways:

1. Distinguishing between a forward and backward transition matrix directed according to the dimension of time was important in the earlier work. Such a distinction is not relevant for the present application in which the forward and backward transition matrix give identical results. This is accomplished by constructing a symmetrical matrix C_1. In this respect, our new approach is similar to those based on a distance-variance matrix of differences between variables measured at a given distance from one another.

2) Our approach is based on spatial correlation parabolas for the 500-, 1000-, and 2000-m neighborhoods (Fig. 6). The "noise" component in each

of the variables is to have been eliminated successfully before spatial factor analysis is applied. However, several inconsistencies in the structure of interrelationships between variables are introduced when a parabola is used as a model. For example, the resulting estimated variance-covariance matrices C_0 and C_1 generally are not positive-definite. In other methods of approach, this problem is avoided by using estimators that are positive-definite. In our study, positive-definiteness of C_0 and C_1 will be imposed by use of an adjustment algorithm (Appendix B). Imposition of the adjustment algorithm ensures positive-definiteness, and comparison of the matrix before and after adjustments indicates that only minor changes to the coefficients occur, thus not greatly changing the correlations between variables.

3. As in ordinary factor analysis, the result of spatial factor analysis, ideally, consists of one or more linear combinations of the variables that reflect one or more independent geological processes. The first spatial factor would have maximum autocorrelation whereas, at the same time, the sum of squared differences between observed and predicted values at a given distance is minimized if the entire transition matrix is used for extrapolation (minimax criterion; Agterberg 1974, p. 467). Quenouille (1957) has shown that, for a first-order Markov scheme in multiple time-series analysis, the first canonical variable (which is equivalent to a spatial factor) has maximum estimated autocorrelation coefficient which is positive and less than one.

However, in practical applications, Quenouille (1957, e.g., his artificial series no. 2, p. 31) found that large positive (>1) or negative (<-1) eigenvalues can occur. These spurious results were caused primarily by approximate linear relationships between variables (Quenouille, 1957, p. 93, 94). Such large positive and negative eigenvalues were encountered in most applications of the model described in this paper. In part, they are caused by lack of precision of the estimator employed. For this reason, each spatial factor must be tested for its goodness of fit in extrapolation.

Application of Spatial Factor Analysis to Four-Component Subsystem CO_2–Li–S–Zn

The method of spatial factor analysis used here is explained initially by using a relatively simple example. The ordinary correlation matrix of the geochemical subgroup consisting of CO_2, S, Li, and Zn in the Ben Nevis area is

$$R = \begin{array}{c|cccc} & CO_2 & S & Li & Zn \\ \hline & 1.00 & -0.03 & 0.56 & 0.13 \\ & -0.03 & 1.00 & 0.04 & 0.05 \\ & 0.56 & 0.04 & 1.00 & 0.23 \\ & 0.13 & 0.05 & 0.23 & 1.00 \end{array}$$

Suppose that estimated values of the constant term a are taken from the best-fitting parabolas for $D = 1$ km. Then, the correlation matrix becomes

R_{01}

CO_2	S	Li	Zn
0.34	0.03	0.30	0.04
0.03	0.31	0.11	0.26
0.30	0.11	0.39	0.23
0.04	0.26	0.23	0.32

R_{01} is not a correlation matrix in the strictest sense because its diagonal elements are not equal to 1. It represents the variance-covariance matrix of signal values corresponding to standardized values of the elements as implied by Eqs. (1)–(5) (Appendix A); the diagonal elements in this array are considerably less than unity, suggesting that the "noise" component of the four variables is considerable. The off-diagonal elements were obtained by averaging the two separate estimates of the cross-correlation function (Table 2). Extrapolation of the cross-correlation function for $D = 1$ km to the origin resulted in correlation coefficients that are either greater or slightly less than the ordinary correlation coefficients. This suggests that the "noise" components of these variables are either positively correlated or not correlated with one another. Part of the noise in the variables can be assumed to be due to measurement errors and these would be uncorrelated. Some local variability may be correlated positively and this is borne out by the preceding comparison. For example, CO_2 and Li have ordinary correlation coefficient equal to 0.56 and an extrapolated value of $a = 0.30$, suggesting that noise $E(N_{1i}N_{2i}) = 0.56–0.30 = 0.26$ (cf. Appendix A). Any pair of the elements taken for this example is not likely to be negatively correlated with one another. The weak negative correlations derived from the slightly negative differences are due probably to sampling fluctuations. A direct measure of the magnitude of these sampling fluctuations is available for cross-correlations. As explained before, off-diagonal elements in matrix R_{01} are averages of values of a for two separate parabolas. The following matrix shows original values of a before averaging

	CO_2	S	Li	Zn
CO_2	0.34	0.01	0.30	−0.01
S	0.04	0.31	0.14	0.23
Li	0.30	0.08	0.39	0.12
Zn	0.08	0.29	0.34	0.32

Elements above the diagonal pertain to the situation where chemical constituents labeling the rows were placed at the centers of the neighborhoods and those labeling the columns at the other points. Elements below the diagonal were obtained by placing chemical constituents for the columns at the centers.

The cross-correlation function for Li and Zn has the largest discrepancy at the origin. The next correlation matrix shows values of a as derived from the best-fitting parabola for $D = 2$ km

$$R_{02} = \begin{array}{cccc} \text{CO}_2 & \text{S} & \text{Li} & \text{Zn} \\ \hline 0.37 & 0.02 & 0.35 & 0.09 \\ 0.02 & 0.21 & 0.05 & 0.19 \\ 0.35 & 0.05 & 0.41 & 0.18 \\ 0.09 & 0.19 & 0.18 & 0.24 \end{array}$$

Correlation coefficients of this new matrix are probably not as good as corresponding values of a in the matrix for the 1000-m neighborhood. This is because the goodness of fit of the parabola decreases toward the origin for larger neighborhoods when D is increased. Nevertheless, values of a in matrices R_{01} and R_{02} are close to one another indicating that both estimates are relatively good. Suppose a correlation matrix R_{11} is formed by taking correlation coefficients from parabolas for the $D = 1000$-m neighborhood at a distance 500 m from the origin

$$R_{11} = \begin{array}{cccc} \text{CO}_2 & \text{S} & \text{Li} & \text{Zn} \\ \hline 0.32 & 0.04 & 0.33 & 0.13 \\ 0.04 & 0.07 & 0.02 & 0.03 \\ 0.33 & 0.02 & 0.34 & 0.11 \\ 0.13 & 0.03 & 0.11 & 0.06 \end{array}$$

The sampling fluctuations of elements of R_{11} are probably less than those of R_{01}. This is indicated by the following matrix, which is based on two separate parabolas before averaging

	CO_2	S	Li	Zn
CO_2	0.32	0.04	0.33	0.13
S	0.03	0.07	0.02	0.03
Li	0.33	0.02	0.34	0.11
Zn	0.13	0.05	0.11	0.06

Off-diagonal elements for separate parabolas in this matrix are nearly equal to one another.

In analogy with previous methods (Agterberg 1974; Royer 1984), the non-symmetric transition matrix U which satisfies

$$U = R_{01}^{-1} R_{11} \tag{1}$$

can be formed. The underlying statistical model is

$$Z_i' = Z_j' U + E_i' \tag{2}$$

where Z_i' and Z_j' are row vectors consisting of standardized values for the four variables at points i and j; E_i is a row vector consisting of residuals. Let S_j represent a column vector for signal values corresponding to Z. Then, premultiplication of both sides of Eq. (2) by S_j yields

$$S_j Z_i' = S_j Z_j' U + S_j E_i'.$$

If expected values are taken, the second term on the right side of this expression disappears and Eq. (1) follows from $R_{11} = R_{01} U$. Each column of U would represent a set of regression coefficients by which the value of a variable at point i is predicted from values of all variables at point j. Suppose that the residual variance for variable Z_k is written as σ_k^2. If the approach is valid, the kth column of U would have $\sigma_k^2 R_{01}^{-1}$ as its variance-covariance matrix, with

$$R_{01}^{-1} = \begin{matrix} -10.4 & 12.2 & 16.5 & -20.3 \\ 12.2 & -1.1 & -14.8 & 10.0 \\ 16.5 & -14.8 & -20.3 & 24.5 \\ -20.3 & 10.0 & 24.5 & -20.1 \end{matrix}$$

Variances of the variables are proportional to elements along the main diagonal of this matrix. They would be negative, indicating that the approach does not give valid results. The reason for negative variances is that R_{01} has a negative eigenvalue in violation of the condition that it should be positive-definite. In other attempted applications, similar violations of the condition of positive-definiteness for both R_{0j} and R_{1j} were found. The subscript in these expressions is related to the type of neighborhood used for evaluation, e.g., $j = 1$ for $d = 500$ m, $D = 1000$ m. However, the negative eigenvalues of the R_{ij} matrices ($i = 0$ or 1) were small and a simple adjustment could be made. Appendix B outlines the adjustment algorithm that was applied to give the matrix R_{ij}' a positive-definite characteristic. For the present example, the eigenvalues of R_{01} were

$$0.842 \quad 0.437 \quad 0.096 \quad -0.015$$

The sum of these values is Trace $(R_{01}) = 1.360$. Consequently, -0.015 was replaced by 0.014. The new matrix R_{01} is

$$R_{01} = \begin{array}{cccc} \text{CO}_2 & \text{S} & \text{Li} & \text{Zn} \\ \hline 0.34 & 0.02 & 0.29 & 0.04 \\ 0.02 & 0.31 & 0.11 & 0.25 \\ 0.29 & 0.11 & 0.40 & 0.22 \\ 0.04 & 0.25 & 0.22 & 0.33 \end{array}$$

This positive-definite matrix is only slightly different from the previous matrix R_{01}. However, its inverse R_{01}^{-1}, which also has become positive-definite,

has changed considerably

$$R_{01}^{-1} = \begin{array}{|cccc|}\hline \text{CO}_2 & \text{S} & \text{Li} & \text{Zn} \\ \hline 19.0 & -7.9 & -21.1 & 17.4 \\ -7.9 & 12.6 & 10.7 & -15.6 \\ -21.1 & 10.7 & 27.6 & -23.6 \\ 17.4 & -15.6 & -23.6 & 28.1 \\ \hline \end{array}$$

Application of the adjustment algorithm to R_{11} gave

$$R_{11} = \begin{array}{|cccc|}\hline \text{CO}_2 & \text{S} & \text{Li} & \text{Zn} \\ \hline 0.33 & 0.04 & 0.32 & 0.13 \\ 0.04 & 0.07 & 0.02 & 0.03 \\ 0.32 & 0.02 & 0.35 & 0.12 \\ 0.13 & 0.03 & 0.12 & 0.07 \\ \hline \end{array}$$

The new transition matrix $U = R_{01}^{-1}R_{11}$ is

$$U = \begin{array}{|cccc|}\hline \text{CO}_2 & \text{S} & \text{Li} & \text{Zn} \\ \hline 1.33 & 0.38 & 0.76 & 0.82 \\ -0.63 & 0.26 & -0.47 & -0.35 \\ -0.56 & -0.36 & 0.16 & -0.63 \\ 1.06 & 0.09 & 0.50 & 0.78 \\ \hline \end{array}$$

All elements of this matrix have positive variances. Note that Eq. (1) implies

$$Z_j' = Z_i' U + E_j' \tag{3}$$

because R_{11} is symmetrical. Equation (3) states that the transition matrix for predicting from point i to j is the same as that for predicting from point j to i. Another property of U is that all eigenvalues are real (positive or negative numbers) because it is the product of two positive-definite matrices (Bellman, 1960, p. 67).

The number of coefficients in U is equal to p^2 being the square of the number of variables p. This number can be reduced by decomposition of U into p separate spectral components $U_i = \lambda_i V_i T_i'$ $(i = 1, 2, \ldots, p)$ with

$$U = \sum_{i=1}^{p} U_i = \sum_{i=1}^{p} \lambda_i V_i T_i'$$

and retaining only one or a few of these components. The largest eigenvalue (λ_1) of U represents a "spatial factor" with scores $Z_i' V_1$, where V_1 is the eigenvector of U corresponding to λ_1. V_1 is one of the columns of V with

$$U'V = VL$$

where L is the diagonal matrix of the eigenvalues of U. For the case of four variables and a neighborhood of $D = 1000$ m, $d = 500$ m, eigenvalues are

$$1.292 \quad 0.827 \quad 0.372 \quad 0.031$$

Each of these corresponds to a linear relationship between the variables. Ideally, the relative importance of a relationship is controlled by the magnitude of its eigenvalue. Here

$$Z_i' V_1 = 0.553z_1 - 0.310z_2 - 0.504z_3 + 0.587z_4$$

where z_1, z_2, z_3, and z_4 represent standardized CO_2, S, Li, and Zn values, respectively. Each of these elements describes a pattern proportional to that of the scores ($Z_i' V_1$). Constants of proportionality or amplitudes are given by the "amplitude vector" T_1', which is a row of the matrix $T = V^{-1}$. For the example

$$T_1' = (2.644, 0.319, 2.223, 1.289)$$

The first and third coefficient of this amplitude vector are largest, indicating that the first spatial factor is primarily for CO_2 and Li. The second eigenvalue ($\lambda_2 = 0.827$) is not much smaller than λ_1. Its spatial factor is

$$Z_i' V_2 = -1.162z_1 - 0.430z_2 - 2.216z_3 + 1.545z_4$$

with amplitudes

$$T_2' = (0.631, -0.257, 0.465, 0.351)$$

The second spatial factor, therefore, is also primarily for CO_2 and Li. It provides a refinement of the pattern provided by the first spatial factor.

A reason for adopting the preceding approach of spectral decomposition of the transition matrix is as follows. Suppose that U is replaced by its first dominant component

$$U_1 = \lambda_1 V_1 T_1'$$

This relationship would apply to points which are $d = 1$ km apart. For points which are d km apart, the corresponding transition matrix is

$$U_1^d = \lambda_1^d V_1 T_1'$$

When d is increased, U^d approaches U_1^d in all applications. Normally λ_1 and other eigenvalues of U are expected to be less than unity as in the situation of a first-order Markov scheme (cf., Quenouille, 1957). In this example, our initial estimate of $\lambda_1 = 1.292$ is too large. For $d = 0$, which is equivalent to extrapolation toward the origin, Eq. (4) reduces to

$$U_1^0 = V_1 T_1'$$

If two eigenvalues are much larger than the others, as in the present example, this approach leads to

$$U_{12}^0 = U_1^0 + wU_2^0 = V_1T_1' + wV_2T_2'$$

where $w = \lambda_1/\lambda_2$ is a weighting factor reducing the relative influence of U_2^0 with respect to U_1^0. In the example $w = 0.640$. The spatial factor for $Z_i'V_1$ is shown (Fig. 7a). Patterns for the first two spatial factors represent carbonate alteration zones. Later, $\lambda_1 = 1.292$ is shown to indeed be a poor estimate of the largest eigenvalue and U_1 is shown to be improved by replacing it by $U_1^* = c_1U_1$ where c_1 is a constant ($c_1 = .475$ for this example). Even if λ_1 cannot be estimated with precision, $Z_i'V_1$ still provides the pattern of the first spatial factor, whereas coefficients of T_1' provide relative amplitudes by which variables describe this pattern. Similar modifications can be applied to other components or sums of components such as $U_1 + U_2$ in the present example.

The preceding experiment was repeated by using R_{02} and constructing R_{12} from the estimated auto- and cross-correlation functions for $D = 2000$ m with $d = 1000$ m. This led to a transition matrix with eigenvalues

$$2.196 \quad 0.685 \quad 0.392 \quad 0.022$$

The first eigenvalue is much larger than the others. The corresponding spatial factor is

$$Z_i'V_1' = 0.356z_1 - 0.480z_2 - 0.506z_3 + 0.622z_4$$

with amplitudes

$$T_1' = (0.124, -1.604, 0.164, 0.434)$$

Without further analysis, this might suggest that in prediction from $d = 1000$ m, sulfur dominates. However, this is not true (shown later). On the other hand, the second eigenvalue ($\lambda_2 = 0.685$) has spatial factor

$$Z_i'V_2 = 1.157z_1 + 0.1172z_2 + 0.124z_3 + 0.054z_4$$

which is comparable to the first spatial factor of the 1000-m neighborhood. The pattern of $Z_i'V_2$ for the 2000-m neighborhood is shown (Fig. 7b). Its amplitudes

$$T_2' = (-0.762, -0.100, -0.753, -0.254)$$

also shows that this trend factor represents carbonate alteration.

The squared multiple correlation coefficient R_{km}^2 can be used to evaluate the relative predictive power of the kth spatial factor for the mth variable in comparison with other spatial factors. This will permit identification of spurious results such as those related to the largest eigenvalue for the $D = 2000$-m neighborhood. Each signal component S_m initially has variance a_m. Therefore, with

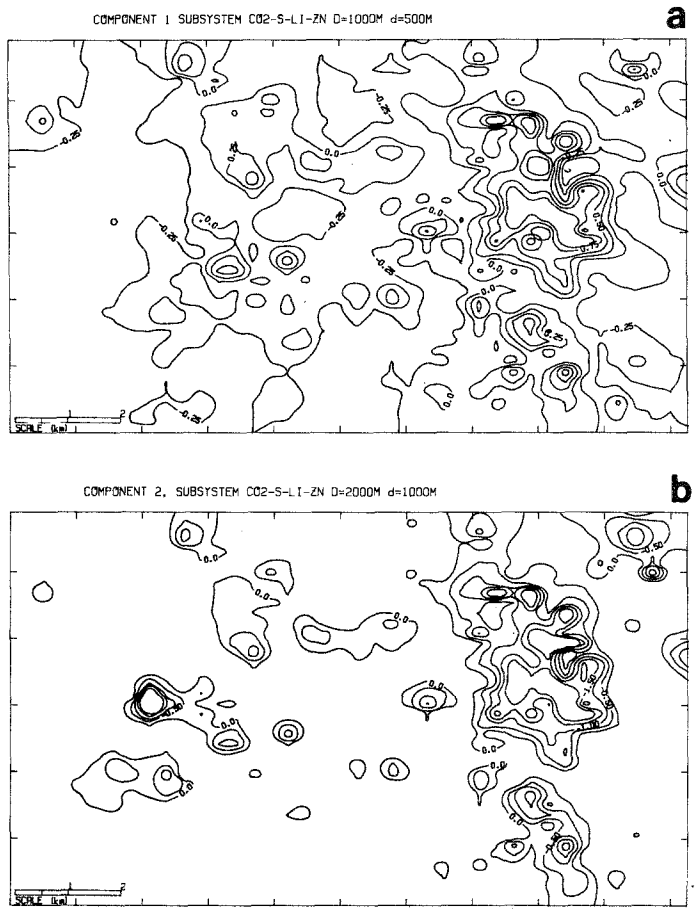

Fig. 7. (a) Spatial factor map of the first component of the U transition matrix (CO_2, S, Li, Zn) evaluated from cross- and auto-correlation functions in the 1000 m neighborhood. (b) Spatial factor map of the second component of the U transition matrix (CO_2, S, Li, Zn) evaluated from cross- and auto-correlation functions in the 2000 m neighborhood. The pattern reflects zones of carbonatization and sulfide mineralization.

p variables, the total variation in the system is equal to

$$T = \sum_{m=1}^{p} a_m$$

For prediction of S_m at point i from all p variables at point j

$$\underset{mi}{\hat{s}} = Z_j' U_m$$

where U_m represents the mth column of U. If R_{1m} is the mth column of R_1, the squared multiple correlation coefficient R_m^2 for predictive power with respect to the mth variable (c.f., Rao, 1975, p. 266) satisfies

$$R_m^2 = R_{1m}' U_m / a_m$$

Total predictive power of U can be expressed by means of the quantity Q

$$Q = \sum_{m=1}^{p} a_m R_m^2 / T$$

For example, the transition matrix U for the $D = 1000$-m neighborhood has

$$R_1^2 = 1.050 \quad R_2^2 = 0.097 \quad R_3^2 = 0.876 \quad R_4^2 = 0.211 \quad \text{and}$$

$$Q = 0.587$$

Note that R_1^2 is slightly greater than one which is its theoretically largest value. No attempt was made to adjust the model in order to avoid this minor discrepancy.

The first component U_1 for this example satisfies

$U_1 =$

CO_2	S	Li	Zn
1.89	0.23	1.59	0.92
−1.06	−0.13	−0.89	−0.52
−1.72	−0.21	−1.45	−0.84
2.01	0.24	1.67	0.98

Comparison of U_1 to U indicates that values of U_1 should be divided by a constant c_1 in order to obtain values of U_1 which are relatively close to values of U. The initial discrepancy between U_1 and U may be due to imprecision of our initial estimate of eigenvalue λ_1. Suppose that constant c_1 is estimated by minimizing the expression

$$\sum_{ij} (U_{ij} - c_1 U_{1ij})^2$$

This leads to the solution

$$c_1 = \sum (U_{ij} U_{1ij} \Big/ \sum U_{1ij}^2$$

For the example $c_1 = 0.4745$, multiplication of $\lambda_1 = 1.292$ by c_1 would give a modified eigenvalue $\lambda_1^* = 0.613$, which is less than one. The modified

first component $U_1^* = c_1 U_1$ satisfies

$$U_1^* = \begin{array}{cccc} \text{CO}_2 & \text{S} & \text{Li} & \text{Zn} \\ \hline 0.90 & 0.11 & 0.75 & 0.44 \\ -0.50 & -0.06 & -0.42 & -0.24 \\ -0.82 & -0.10 & -0.69 & -0.40 \\ 0.95 & 0.11 & 0.80 & 0.46 \end{array}$$

This matrix shows good agreement with U. In terms of squared multiple correlation coefficients, the first component U_1^* has R^2 coefficients equal to

$$R_{11}^2 = 0.380 \quad R_{12}^2 = 0.006 \quad R_{13}^2 = 0.230 \quad R_{14}^2 = 0.094 \quad \text{and}$$

$$Q_1 = 0.185$$

Correction constants c_i $(i = 1, 2, \ldots, p)$ can be estimated for all components. The second component has $c_2 = -0.431$ and its structure is such that all squared multiple correlation coefficients resulting from it would be negative, indicating that U_2^* alone cannot be used for prediction. However, addition of U_2 to U_1 gives U_{12} with $c_{12} = 0.903$ and

$$U_{12}^* = \begin{array}{cccc} \text{CO}_2 & \text{S} & \text{Li} & \text{Zn} \\ \hline 1.17 & 0.30 & 0.68 & 0.74 \\ -0.76 & -0.15 & -0.52 & -0.43 \\ -0.53 & -0.38 & 0.13 & -0.59 \\ 1.09 & 0.35 & 0.52 & 0.77 \end{array}$$

which is close to U. Its squared multiple correlation coefficients are

$$R_{121}^2 = 0.935 \quad R_{122}^2 = 0.019 \quad R_{123}^2 = 0.788 \quad R_{124}^2 = 0.185 \quad \text{and}$$

$$Q_{12} = 0.508$$

Although the addition of U_2 to U_1 increases these values, the overall patterns are not changed greatly, as pointed out before.

Application of the preceding method to the first two spatial factors derived from the transition matrix U for the 2000-m neighborhood gave the following results. For U

$$R_1^2 = 0.463 \quad R_2^2 = 0.080 \quad R_3^2 = 0.421 \quad R_4^2 = 0.098 \quad \text{and}$$

$$Q = 0.358$$

This result is comparable with that for the 1000-m neighborhood. However, the first component has $Q_1 = 0.051$, whereas the second component, with $Q_2 = 0.263$, has about five times as much predictive power. This proves that,

although it has the largest eigenvalue, the spatial factor dominated by sulfur is less meaningful than the carbonate alteration factor.

Application of Spatial Factor Analysis to Seven- and Nine-Component Subsystems

In the preceding section, application of the method of spatial factor analysis was restricted to the four variables that describe alteration and mineralization of the area. In particular, variables that were studied tend to be more isotropic in their spatial distribution than variables that define compositional variation. Many of the distinct geological units that reflect primary compositional variation are spatially anisotropic in their patterns (Fig. 2). An obvious case is that of felsic volcanic rocks. This anisotropy is revealed in spatial patterns of chemical variables (Fig. 4a). Also, auto-correlation functions for Si (Fig. 6) and several other variables that reflect compositional variation (not shown) indicate a steep decay of the function as distance increases. This reflects poor auto- and cross-correlation at distances greater than 500 m.

Application of spatial factor analysis to larger groups of seven and nine variables was made using three neighborhoods of $D = 2000$ m, 1000 m, and 500 m. From the discussion of factors that have been determined from correspondence analysis, the spatial factor analysis is expected to reveal the same spatial patterns. In all three neighborhoods for both seven and nine variable sets, R_0 estimates were subjected to small adjustments in order to satisfy the positive-definite condition.

Evaluation of the seven variable case with $D = 2000$ m showed that the R_{01} coefficients are small. This is due to rapid decay with distance of values determined from the auto- and cross-correlation functions for variables that reflect compositional variation. Because of small R_{01} coefficients, the resulting R_{01}^{-1} matrix coefficients are large and the diagonals represent large variances of variables when $D = 2000$ m. When large variances exist, eigenvalue solutions will not be valid and may be large. Similarly, for the neighborhood $D = 1000$ m, $d = 500$ m, although eigenvalues were more realistic, the factor patterns were difficult to interpret. Large neighborhoods (1000 m and 2000 m) yield small Q values when subjected to spatial factor analysis.

For the neighborhood $D = 500$ m, $d = 250$ m, eigenvalues were 3.721, 1.560, 0.590, 0.503, 0.281, 0.231, 0.114, and $Q = 0.608$, which is a prediction of spatial relationships. R^2 values were 0.717, 0.704, 1.306, 0.425, 0.578, 0.341, and 0.770. Only two components of U are interpretable ($Q > 0$) and are

$R^2 =$

C#	Q	1	2	3	4	5	6	7
1	0.176	0.001	0.471	0.001	0.019	0.216	0.109	0.234
2	0.263	0.583	0.005	0.881	0.323	0.187	0.001	0.400

The corresponding amplitude vectors for these two components are

$$T_1' = (-0.0586 \quad -1.5817 \quad 0.0392 \quad 0.2925 \quad -1.0702 \quad -0.8306 \quad 1.1066)$$

$$T_2' = (1.2392 \quad -0.1404 \quad -1.2929 \quad -1.0987 \quad -0.9049 \quad -0.0678 \quad 1.3157)$$

The value of Q for the second component suggests that it is more significant. The amplitude vector of the second component suggests that the positive trend vector coefficients represent felsic volcanic rocks of which the positive scores are represented by variables K and Si, and the negative scores are represented by variable Fe, Mg, Ca, Al, and Na. Note that the amplitude vector tends to indicate which variables are associated with each other by their sign, whereas the multiple correlation coefficients indicate by their magnitude which variable dominates in the resulting spatial factor pattern.

Spatial factor 2 (Fig. 8a) (when compared to Figs. 2 and 4a) outlines the felsic and mafic volcanic rocks. However, the felsic rock pattern in the northwest and north central part of the map area is not the same (Figs. 8a and 4a), which is due probably to relatively thin volcanic units (much less than 500 m thick). The existence of these units cannot be detected in the auto- and cross-correlation functions.

Factor 1 indicates that (Al, Ca, and Na) and (Si) are the most significant variables associated with negative factor scores and that K, Mg, and Fe are associated with positive factor scores. The resulting spatial factor map (not shown) indicates that negative scores are associated with compositional variation of volcanics and positive scores are associated with K alteration.

The spatial factor analysis was applied to the nine-variable set of data with the following neighborhoods, $D = 2000$ m, $d = 1000$ m; $D = 2000$ m, $d = 500$ m; and $D = 1000$ m, $d = 500$ m.

From results of spatial factor analysis applied to the seven- and four-variable sets of data, similar results can be expected to be obtained and factors probably will be a combination of the other two applications. For $D = 2000$ m, $d = 1000$ m, little information of the compositional variation was expected but carbonate alteration patterns should be detected. In this analysis

$$Q = 0.2623$$

and R^2 coefficients were

	1	2	3	4	5	6	7	8	9
$R^2 =$	0.105	0.267	0.141	0.117	0.159	0.024	0.105	0.592	0.639

From these coefficients, clearly CO_2 and Li dominate the spatial factors.

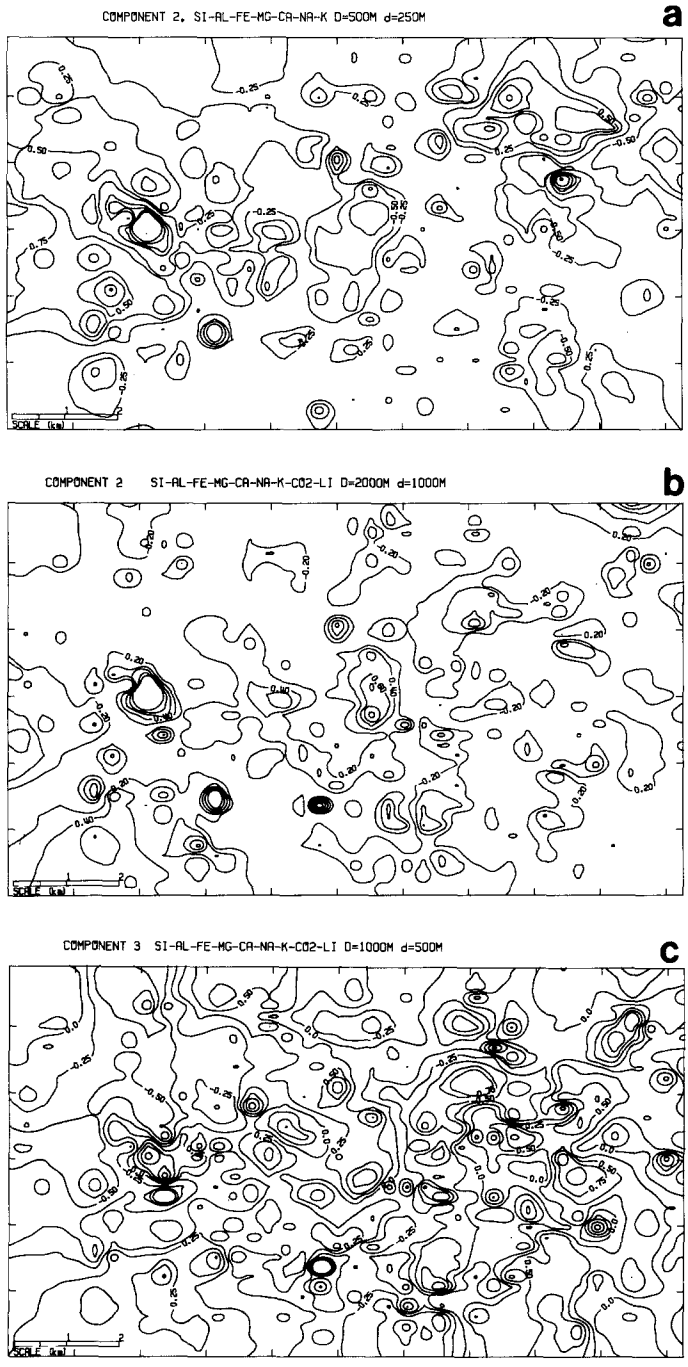
COMPONENT 2. SI-AL-FE-MG-CA-NA-K D=500M d=250M
a
COMPONENT 2 SI-AL-FE-MG-CA-NA-K-CO2-LI D=2000M d=1000M
b
COMPONENT 3 SI-AL-FE-MG-CA-NA-K-CO2-LI D=1000M d=500M
c

The following components were significant in the analysis

	C#	Q	1	2	3	4	5	6	7	8	9
R^2	1	0.024	0.032	0.018	0.028	0.051	0.019	0.011	0.000	0.059	0.012
	2	0.055	0.000	0.007	0.028	0.007	0.000	0.002	0.022	0.112	0.226
	4	0.010	0.000	0.023	0.002	0.006	0.015	0.000	0.000	0.012	0.025
	5	0.019	0.053	0.005	0.050	0.025	0.018	0.000	0.056	0.001	0.004

with amplitude vectors

$$T'1 = (0.571, 0.522, 0.528, 0.777, 0.528, 0.507, -0.003, -1.064, -0.503)$$

$$T'2 = (-0.007, -0.295, 0.481, 0.259, -0.046, 0.186, 0.562, -1.341, -1.999)$$

$$T'4 = (-0.003, -0.587, 0.140, 0.280, -0.474, -0.064, -0.061, 0.501, 0.753)$$

$$T'5 = (-0.513, 0.184, 0.496, 0.375, 0.353, 0.009, -0.694, 0.073, 0.192)$$

The first component appears to be dominated by Mg, Si, Fe, Al, Ca, and Na for positive factor scores and by CO_2, Li, and K for negative factor scores. Positive scores reflect compositional variation of the volcanics combined with zones of alteration associated with CO_2, Li, and K enrichment.

The second component has the largest Q value and R^2 coefficients; together with the amplitude vector coefficients, this indicates that Li and CO_2 dominate this spatial factor also. The spatial plot of factor 2 (Fig. 8b) indicates Li and CO_2 patterns are not clearly developed. In fact, the pattern is similar locally to the Ca pattern (Fig. 4b), although the R^2 coefficient for Ca in the second component is equal to zero. This pattern also is similar to the third factor of the correspondence analysis applied to nine variables. The third factor in correspondence analysis is dominated by CO_2 and Ca together, which may have good spatial cross-correlation and result in the pattern observed in the spatial factor analysis. The reason for this is difficult to interpret. The poor result may be a combination of a small Q value ($Q = 0.055$), which suggests that the factor is not strong. Contrary to this, the first component, which has only half the pre-

Fig. 8. (a) Spatial factor map of the second component of the U transition matrix (Si-Al-Fe-Mg-Na-K) evaluated from auto- and cross-correlation functions in the 500 m neighborhood. (b) Spatial factor map of the second component of the U transition matrix (Si-Al-Fe-Mg-Ca-Na-K-CO_2-Li) evaluated from auto- and cross-correlation functions in the 2000 m neighborhood. (c) Spatial factor map of the third component of the U transition matrix (Si-Al-Fe-Mg-Ca-Na-K-CO_2-Li) evaluated from auto- and cross-correlation functions in the 1000 m neighborhood.

dictive power, produces the primary compositional variation and alteration patterns. Another reason why the pattern does not appear could be the lack of precision of the R_0 and R_1 matrices at $d = 1000$ m for $D = 2000$ m. Whereas these matrices could be estimated with sufficient precision in the four-variable case, they cannot be in the seven-variable case. Results for the nine-variable case are only partly interpretable for this neighborhood.

The fourth and fifth components have small Q values and their patterns do not appear to have any significant meaning. For the case of $D = 2000$ m, $d = 500$ m, $Q = 0.446$ and

	1	2	3	4	5	6	7	8	9
$R^2 =$	0.256	0.515	0.282	0.254	0.374	0.171	0.314	0.795	0.814

	Q	1	2	3	4	5	6	7	8	9
$R^2 =$	1	0.052	0.001	0.010	0.020	0.030	0.003	0.003	0.000	0.145	0.178
	2	0.023	0.001	0.045	0.006	0.002	0.019	0.035	0.021	0.013	0.035
	4	0.045	0.101	0.011	0.046	0.043	0.015	0.018	0.175	0.003	0.023
	5	0.015	0.017	0.002	0.042	0.004	0.058	0.008	0.017	0.001	0.008

The corresponding amplitude vectors are

$$T_1' = (-0.140, 0.449, -0.530, -0.712, -0.242, -0.330, 0.075, 1.990, 2.320)$$

$$T_2' = (0.229, -1.954, 0.595, -0.383, -1.230, -2.172, 1.454, 1.212, 2.048)$$

$$T_4' = (-0.939, 0.370, 0.630, 0.657, 0.433, 0.613, -1.629, 0.207, 0.656)$$

$$T_5' = (-0.535, 0.237, 0.833, 0.261, 1.176, -0.561, -0.708, -0.175, -0.517)$$

The first component has the largest Q value; however, the spatial pattern is similar to that of $D = 2000$ m, $d = 1000$ m of the second factor. Negative scores for CO_2 and Li show the zones of alteration throughout the area. Positive scores are dominated by Mg-rich zones. The fourth component is the next largest component, and from both amplitude vector and R^2 coefficients, K appears to be the dominant variable.

For the case of $D = 1000$ m and $d = 500$ m, $Q = 0.432$

	1	2	3	4	5	6	7	8	9
$R^2 =$	0.103	0.488	0.265	0.196	0.202	0.252	0.274	1.158	0.989

The most significant components are

Q	1	2	3	4	5	6	7	8	9
0.045	0.006	0.093	0.013	0.070	0.007	0.051	0.098	0.013	0.025
0.069	0.001	0.049	0.002	0.007	0.002	0.111	0.066	0.214	0.138
0.076	0.002	0.116	0.060	0.016	0.041	0.001	0.003	0.275	0.205
0.005	0.012	0.002	0.012	0.009	0.006	0.000	0.007	0.000	0.001

and amplitude vectors are

$$T_1' = (-0.241, 1.074, -0.317, -0.865, 0.307, 0.917, -1.202, 0.381, 0.560)$$

$$T_2' = (0.081, -0.698, 0.119, -0.237, -0.137, -1.209, 0.885, 1.362, 1.1720)$$

$$T_3' = (-0.158, -1.281, 0.726, 0.443, -0.810, -0.124, -0.238, 1.841, 1.7040)$$

$$T_5' = (1.342, -0.565, -1.247, -1.226, -1.173, 0.185, 1.277, 0.2356, -0.4878)$$

The third component is most significant, with the largest Q value. R^2 and amplitude vector coefficients indicate that CO_2 and Li are the most significant variables. A spatial plot of the third factor (Fig. 8c) clearly shows that the CO_2–Li enriched zones are indicated in the pattern. The negative factor score pattern is associated with the zone of Ca enrichment around the CO_2–Li zone. The fifth component is dominated by Si and K for positive factor scores and a combination of Fe, Mg, and Ca for the negative factor scores; the spatial pattern is similar to the Si map (Fig. 4a). The second component appears to be a combination of CO_2 and Ca together, as defined in the correspondence analysis. The first component is a combination of Si, Fe, Mg, and K for negative factor scores and Al, Ca, Na, CO_2, and Li for positive factor scores, outlining both compositional variation and alteration zones.

Results for the nine-variable subsystem at $d = 500$ m, $D = 1000$ m are similar to those previously described for the four-variable subsystem at $d = 500$ m, $D = 1000$ m, as well as $d = 1000$ m, $D = 2000$ m in that the dominant trend factor is controlled primarily by CO_2 and Li representing the carbonate alteration.

CONCLUDING REMARKS

Correspondence analysis gives useful results for the Ben Nevis area including a carbonate alteration factor, which is characterized mainly by CO_2. The first factor emerging in correspondence analysis, as well as in other types of factor analysis, is the compositional trend of volcanics ranging from basalts to rhyolites. This lithologic trend is described by SiO_2 and most other chemical constituents.

Spatial variation of constituents was studied by fitting parabolas to auto- and cross-correlation functions for overlapping neighborhoods. This suggests the existence of exponential-type auto- and cross-correlation functions with discontinuous first derivative at the origin for most chemical constituents. However, CO_2 and Li have Gaussian-type auto-correlation functions with continuous first derivative at the origin. Their cross-correlation function suggests the existence of a local minimum at the origin. The latter pattern is to a lesser extent exhibited by cross-correlation of these two elements with S and Zn. Spatial correlation patterns of constituents that resulted primarily from hydrothermal alteration processes may be concluded to differ from those of other chemical constituents. A method of spatial factor analysis was applied to three subsystems which include variables that describe compositional variation, variables that describe alteration, and a combination of both sets of variables.

Primarily because of instability of estimated eigenvalues, great care is required in interpreting the results. Nevertheless, results of the spatial factor analysis can be interpreted when auto- and cross-correlation functions represent meaningful relationships between variables at a given neighborhood size.

For variables that represent alteration, the 2000 m and 1000 m neighborhoods define these zones. The pattern of a combination of CO_2–S–Li–Zn enrichment (Fig. 7b) is significant in terms of mineralization and choice of exploration targets. For variables that represent compositional variation, larger neighborhoods do not describe compositional variation well or, in one case, not at all. The degree of anisotropy has an effect on the ability to determine relationships between variables in spatial factor analysis; this was shown by thin units of felsic volcanic rocks not being delineated in the analysis, in the case of $D = 500$ m, $d = 250$ m.

Of particular use are values of Q for the U transition matrix that indicate the ability of U to account for spatial variation in the data. Also, Q_m values estimate the relative significance of components of U and enable an assessment of the most significant factors. Multiple correlation coefficients describe the relative significance of variables for a given component; when used in conjunction with coefficients of the amplitude vector T', spatial patterns can be interpreted and related to the geology of the area.

Spatial factor analysis as used in this paper is suitable for delineation of

hydrothermal alteration patterns and other geological patterns that are characterized by gradational variation in space.

APPENDIX A

Derivation of auto- and cross-correlation functions is based on the equation

$$x_i = F(d_{ij})x_j + y_i \tag{A1}$$

where x_i and x_j denote values of a random variable X with zero mean measured at two different points in the plane labeled i and j. Both i and j go from 1 to N, where N denotes total number of observations. $F(d_{ij})$ is a quadratic function of distance d_{ij} between these two points. The residual y_i is the realization of a random variable y_i at point i. It satisfies $E(Y_i) = 0$, and Y_i is assumed to be independent of X_j. Under these conditions

$$F(d_{ij}) = E(X_iX_j)/E(X_j^2) = \rho_{ij} \tag{A2}$$

where E denotes expected value and ρ_{ij} is the auto-correlation coefficient for two points that are distance d_{ij} apart. Suppose that X_i is replaced by $Z_i = \mathrm{X}_i/\sigma$, where σ is the standard deviation of the variable considered. Let σ be replaced by s representing the standard deviation estimated from N values of x_i, then values of z_i satisfy $z_i = x_i/s$. This rescaling does not change results for auto-correlation, but the model now can be used also for estimating the spatial cross-correlation coefficient of two standardized random variables Z_{1i} and Z_{2j} with values z_{1i} and z_{2j}. In practice

$$F_D(d_{ij}) = a + b\,d_{ij} + c\,d_{ij}^2 \tag{A3}$$

is estimated by ordinary least squares after successively pairing each point labeled i ($i = 1, 2, \ldots, N$) with the N_i points (j) located within a circular neighborhood around i with radius D.

In cross-correlation, either values z_{1i} or z_{2i} can be selected at the centers of neighborhoods. Consequently, two parabolas can be fitted in that situation. The expected parameters a, b, and c of these two parabolas are equal to one another. For this reason, the two fitted parabolas can be averaged in practice. Jointly, the fitted parabolas for different values of D provide an approximation of an auto- or cross-correlation function. By means of this method, Z_i may be divided into "signal" S_i and "noise" N_i components with

$$E(Z_i^2) = E(S_i^2) + E(N_i^2) = 1$$

$$E(Z_iZ_j) = E(S_iS_j) = E(Z_iS_j) = E(S_iZ_j) \quad \text{if} \quad i \neq j \tag{A4}$$

with $Z_i = S_i + N_i$ and $E(S_i^2) = a$. Corresponding equations for a pair of standardized variables Z_1 and Z_2 are

$$E(Z_{1i}Z_{2i}) = E(S_{1i}S_{2i}) + E(N_{1i}N_{2i}) = \rho_{12}$$

$$E(Z_{1i}Z_{2j}) = E(S_{1i}S_{2j}) = E(Z_{1i}S_{2j}) = E(S_{1i}Z_{2j}) \quad \text{if} \quad i \neq j \quad \text{(A5)}$$

where ρ_{12} represents the correlation coefficient of X_1 and X_2, and $E(S_{1i}S_{2i}) = a \neq \rho_{12}$ allows for the possibility that the noise of X_1 is correlated with the noise of X_2.

A basic property of the auto-correlation function is that it is symmetric about its origin. In this paper, this property is assumed to hold true for the cross-correlation function as well.

The parabolas (Fig. 6) and coefficients (Table 2) provide approximations of unknown auto- and cross-correlation functions. Locally these estimates violate basic properties of such functions. For example, an autocorrelation function has its maximum value at the origin. This is a consequence of the so-called Schwarz–Cauchy inequality. Another consequence of this inequality is that the absolute value of a cross-correlation coefficient is not greater than the geometric mean of the autocorrelation coefficients of the two variables considered. The Schwarz–Cauchy inequality is not everywhere satisfied by the parabolas (Fig. 6).

APPENDIX B

Matrices R_{0j} and R_{1j} should be positive-definite (Journel and Huijbregts, 1978, p. 326). A necessary and sufficient condition that a symmetric matrix is positive-definite is that all its eigenvalues are greater than zero (Bellman, 1960, p. 54). As illustrated by the example in the text, the condition of positive-definiteness is not necessarily satisfied if the auto- and cross-correlation coefficients are taken from best-fitting parabolas as in this paper.

If R_{0j} or R_{1j} have one or more small negative eigenvalues, these can be replaced by small positive eigenvalues with the same eigenvectors, provided that the resulting changes of the elements of R_{0j} or R_{1j} are small. In this adjustment algorithm, all eigenvalues of a symmetric matrix R_{ij} ($i = 0$ or 1) are checked for being positive. A negative eigenvalue is replaced by a positive number equal to 0.01 × trace (R_{ij}). This will change the value of Tr (R_{ij}). If another eigenvalue is negative, it will be replaced in the same way using 1% of the modified trace. After adjustment, all eigenvalues of the modified matrix R_{ij} are greater than zero. This implies that R_{ij} has become positive-definite.

Use of this technique in our experiments indicated that adjustments to the R_{0j} and R_{1j} matrices were small. Adjustments to the matrix elements were typically ± 0.01, which averages to about a 3% change in the values and indicates that the fundamental relationships between the variables are unchanged.

LIST OF SYMBOLS

c_i	Scalar factor that minimizes the discrepancy between and U_i.
D	Radius of circular neighborhood used for estimating auto- and cross-correlation coefficients.
d	Distance for which transition matrix U is estimated.
d_{ij}	Distance between observed values i and j.
E	Expected value.
E_i	Row vector of residuals in the standardized model.
$F(d_{ij})$	Quadratic function of distance d_{ij} $F(d_{ij}) = a + bd_{ij} + cd_{ij}^2$
L	Diagonal matrix of the eigenvalues of U.
λ_i	Eigenvalue of the matrix U; ith diagonal element of L.
N	Number of observations.
p	Number of variables.
Q	Total predictive power of U.
R	Correlation matrix of the variables.
R_{0j}	Variance-covariance signal matrix of the standardized variables at origin; j is the index related to d and D (e.g., $j = 1$ for $d = 500$ m, $D = 1000$ m).
R_{1j}	Matrix of auto- and cross-correlation coefficients evaluated at a given distance within the neighborhood.
R_m^2	Multiple correlation coefficient squared for the mth variable.
S_i	Column vector i of the signal values.
s_k^2	Residual variance for variable k.
T_i'	Amplitude vector corresponding to V_i; ith row of $T = V^{-1}$.
T	Total variation in the system.
U	Nonsymmetric transition matrix formed by post-multiplying R_{01}^{-1} by R_{ij}.
U_i	Component i of the matrix U, corresponding to the ith eigenvector V_i; $U_i = \lambda_i V_i T_i$.
U_i^*	Component U_i multiplied by c_i.
U_{ij}	Sum of components $U_i + U_j$.
V_i	Eigenvector of the matrix U; ith column of V with $U'V = VL$.
w	Weighting factor; equal to the ratio of two eigenvalues.
X_i	Random variable at point i.
x_i	Value of random variable at point i.
y_i	Residual of x_i.

Z_i' Row vector i for the standardized variables.

z_i Standardized value of variable.

ACKNOWLEDGMENTS

This project has been funded by the Northern Ontario Geological Survey program of the Ontario Ministry of Northern Development and Mines and is published by permission of Dr. V. G. Milne, Director, Ontario Geological Survey. The research for this study was carried out while E. C. Grunsky was a graduate student at the University of Ottawa, Ontario. This paper is contribution no. 21387 of the Geological Survey of Canada. Thanks are due to C. F. Chung, Geological Survey of Canada, for critical reading of the manuscript.

REFERENCES

Agterberg, F. P., 1966, The Use of Multivariate Markov Schemes in Petrology: Jour. Geol., v. 79, p. 764–785.

Agterberg, F. P., 1970, Autocorrelation Functions in Geology: p. 113–142 in Daniel F. Merriam (Ed.), Geostatistics: Plenum, New York, N.Y.

Agterberg, F. P., 1974, Geomathematics: Elsevier, Amsterdam, 596 p.

Bellman, R., 1960, Introduction to Matrix Analysis: McGraw-Hill, New York, 328 p.

Bennett, R. J., 1979, Spatial Time Series: Pion, London, 674 p.

Delfiner, P., 1976: Linear Estimation of Non Stationary Spatial Phenomena: p. 49–68 *in* Advanced Geostatistics in the Mining Industry, Proceedings of the NATO Advanced Study Institute, M. Guarascio, M. David, and C. Huijbregts (Eds.): D. Reidel Publishing Co., Dordrecht, Holland, 461 p.

Grunsky, E. C., 1986, Recognition of Alteration in Volcanic rocks Using Statistical Analysis of Lithogeochemical Data: Jour. Geochem. Explor., v. 25, p. 157–183.

Haining, R., 1985, Trend surface models with global and local scales of variation: paper originally presented at Conference on Applied Spatial Statistics, Cambridge College of Arts and Technology, April 18, 1985 (to be published in Technometrics).

Huijbregts, C. and Matheron, G., 1971, Universal Kriging (An Optimal Method for Estimating and Contouring in Trend Surface Analysis), *in* Proceedings of the 9th International Symposium on Techniques for Decision-Making in the Mineral Industry; Montreal, June 14–19, 1970; The Canadian Institute of Mining and Metallurgy, Special Volume 12, 507 p.

Jensen, L. S., 1975, Geology of Clifford and Ben Nevis Townships, District of Cochrane: Ontario Division Mines, GR132, 55 p, accompanied by Map 2283, scale 1 in. to $\frac{1}{2}$ mile.

Journel, A. G. and Huijbregts, C. J., 1978, Mining Geostatistics: Academic Press, London, 600 p.

Myers, Donald E., 1982, Matrix Formulation of Co-Kriging: Math Geol., v. 14, p. 249–257.

Myers, Donald E., 1988, Some Aspects of Multivariate Analysis, p. 669–687 *in* Fabbri, A. G., Chung, C. F., and Sinding-Larsen, R. (Eds.), Quantitative Analysis of Mineral and Energy Resources: Proceedings of the NATO Conference, Il Ciocco, Italy, July, 1986; NATO ASI Series C: Math. Phy. Sci., v. 223, D. Reidel Publishing Co., Dordrecht, Holland, 720 p.

Quenouille, M. H., 1968, The Analysis of Multiple Time-series: Hafner, New York, 105 p.

Rao, C. R., 1975, Linear Statistical Inference and Its Applications, 2nd ed. Wiley, New York, 625 p.

Royer, J. J., 1984, Proximity Analysis: A Method for Multivariate Geodata Processing. Application to Geochemical Processing: Sciences de la Terre; Informatique Geologique, no. 20, part 1; Universite de Nancy, France, p. 223–243.

Royer, J. J., 1988, New Approaches to the Recognition of Anomalies in Exploration Geochemistry, p. 89–112, *in*, Fabbri, A. G., Chung, C. F., and Sinding-Larsen, R. (Eds.), Quantitative Analysis of Mineral and Energy Resources: Proceedings of the NATO Conference, Il Ciocco, Italy, July, 1986; NATO ASI Series C: Math. Phy. Sci., v. 223, Reidel, Dordrecht, Holland, 720 p.

Shepard, D., 1968, A Two-Dimensional Interpolation Function for Irregularly Spaced Data: Proceedings of 23rd National Conference, Association for Computing Machinery, Brandon, Princeton, N.J., p. 517–524.

Switzer, P. and Green, A. A., 1984, Min/Max Autocorrelation Factors for Multivariate Spatial Imagery: Technical Report No. 6, April, 1984, Department of Statistics, Standard University, 14 p.

Upton, G. and Fingleton, B., 1985, Spatial Data Analysis by Example; Vol. 1: Wiley, New York, 410 p.

Wackernagel, Hans, 1985, L'Inference d'un mode le lineaire en geostatistique multivariable: Ph.D. thesis, Paris School of Mines.

Wackernagel, Hans, 1988, Geostatistical Techniques for Interpreting Multivariate Spatial Information, p. 393–409 *in* Fabbri, A. G., Chung, C. F., and Sinding-Larsen, R. (Eds.), Quantitative Analysis of Mineral and Energy Resources: Proceedings of the NATO Conference, Il Ciocco, Italy, July, 1986; NATO ASI Series C: Math. Phy. Sci., v. 223, Reidel, Dordrecht, Holland, 720 p.